

Holm oak decline is determined by shifts in fine root phenotypic plasticity in response to belowground stress

Manuel Encinas-Valero¹ , Raquel Esteban² , Ana-Maria Hereş^{1,3} , María Vivas⁴ , Dorra Fakhret⁵ , Iker Aranjuelo⁵ , Alejandro Solla⁴ , Gerardo Moreno⁴  and Jorge Curiel Yuste^{1,6} 

¹BC3-Basque Centre for Climate Change, Scientific Campus of the University of the Basque Country, B/Sarriena s/n, 48940, Leioa, Bizkaia, Spain; ²Department of Plant Biology and Ecology, University of Basque Country (UPV/EHU), B/Sarriena s/n, 48940, Leioa, Bizkaia, Spain; ³Department of Forest Sciences, Transilvania University of Braşov, Sirul Beethoven-1, 500123, Braşov, Romania; ⁴Faculty of Forestry, Institute for Dehesa Research (INDEHESA), Universidad de Extremadura, Avenida Virgen del Puerto 2, 10600, Plasencia, Cáceres, Spain; ⁵Instituto de Agrobiotecnología (IdAB), Consejo Superior de Investigaciones Científicas (CSIC)-Gobierno de Navarra, Avenida Pamplona 123 31192, Mutilva, Spain; ⁶IKERBASQUE – Basque Foundation for Science, Plaza Euskadi 5, E-48009, Bilbao, Bizkaia, Spain

Summary

Author for correspondence:
Manuel Encinas-Valero
Email: encinasvaleromanuel@gmail.com

Received: 27 February 2022
Accepted: 20 April 2022

New Phytologist (2022) 235: 2237–2251
doi: 10.1111/nph.18182

Key words: defoliation, holm oak, nonstructural carbohydrates, phenotypic plasticity, root architecture, soil nutrient availability, trade-off.

- Climate change and pathogen outbreaks are the two major causes of decline in Mediterranean holm oak trees (*Quercus ilex* L. subsp. *ballota* (Desf.) Samp.). Crown-level changes in response to these stressful conditions have been widely documented but the responses of the root systems remain unexplored. The effects of environmental stress over roots and its potential role during the declining process need to be evaluated.
- We aimed to study how key morphological and architectural root parameters and nonstructural carbohydrates of roots are affected along a holm oak health gradient (i.e. within healthy, susceptible and declining trees).
- Holm oaks with different health statuses had different soil resource-uptake strategies. While healthy and susceptible trees showed a conservative resource-uptake strategy independently of soil nutrient availability, declining trees optimized soil resource acquisition by increasing the phenotypic plasticity of their fine root system.
- This increase in fine root phenotypic plasticity in declining holm oaks represents an energy-consuming strategy promoted to cope with the stress and at the expense of foliage maintenance. Our study describes a potential feedback loop resulting from strong unprecedented belowground stress that ultimately may lead to poor adaptation and tree death in the Spanish dehesa.

Introduction

Tree root systems are key components maintaining the functioning and services of forests (Faucon *et al.*, 2017; Freschet & Roumet, 2017). On the one hand, they play an important role in biogeochemical cycling by providing biomass input and mineral nutrients to the soil, through root tissue turnover (Ruess *et al.*, 2003; Brunner & Godbold, 2007; McCormack *et al.*, 2012), and by determining soil structure and stability (Bardgett *et al.*, 2014). On the other hand, roots are also essential for plant fitness and functioning as they are responsible for foraging and transporting water and nutrients (Poorter & Ryser, 2015), providing physical support and storing carbohydrates (Freschet *et al.*, 2021b). However, biotic and abiotic factors determine how roots influence plant and ecosystem functioning (Langley *et al.*, 2006; Berendsen *et al.*, 2012; Bardgett *et al.*, 2014). Investigating the potential risks to which the tree root systems are subjected is thus fundamental for understanding overall ecosystem functioning and stability. In this regard, associations between root traits and

environmental factors make it possible to link root characteristics to a particular process, determine the function of the trait, and evaluate the impact of climate change over plant and ecosystem functioning (Beidler *et al.*, 2015; Faucon *et al.*, 2017; Marañón *et al.*, 2020).

Many biotic factors determine root functioning and functional traits. For instance, mycorrhizal fungi or infection by pathogens may affect root structure (i.e. morphology, architecture) and different aspects of plant physiology (i.e. resource uptake kinetic change, accumulation of phenolic compounds, exudates; Ruíz-Gómez *et al.*, 2015; Freschet *et al.*, 2021a) while plant–plant competition for soil resources may also modify root characteristics (Gea-Izquierdo *et al.*, 2009; Gazol *et al.*, 2021). Also, the soil matrix may strongly affect root functional traits. Contrasting physicochemical soil properties such as texture, water availability, nutrients and/or other factors may modify the architecture, morphology and physiology of the roots (Makita *et al.*, 2011; Alameda & Villar, 2012; Trubat *et al.*, 2012). These modifications represent strategies to optimize the acquisition of resources

when soil environmental conditions become challenging (Bardgett *et al.*, 2014). For instance, root branching may increase in response to soil nutrient hotspots (Mou *et al.*, 2013; Eissenstat *et al.*, 2015; Freschet *et al.*, 2021b), or root diameter and/or length may be altered by soil compaction (Alameda & Villar, 2012) and water availability (Cubera *et al.*, 2012; Brunner *et al.*, 2015). Thus, in response to spatiotemporal soil heterogeneity, roots may exhibit phenotypic plasticity (i.e. different phenotypes) by reflecting differences in their morphology, architecture and/or physiological traits, which result from the interaction between the genotype and the environment (Arnold *et al.*, 2019). This phenotypic plasticity allows roots to maintain their functioning (i.e. resource acquisition) efficiently under challenging environmental conditions. Given that soils are characterized by high spatial heterogeneity, the characterization of the soil properties is critical to capture the variability of intraspecific root functional traits and their link to root functioning (Kumordzi *et al.*, 2019). Although an increasing number of studies have recently focused on root ecophysiology (i.e. root functional traits, roots physiology and soil interaction; Łakomy *et al.*, 2019; Suseela *et al.*, 2020; Freschet *et al.*, 2021b) many gaps remain in our understanding of root functioning under field conditions.

The effects of climate on the functioning of the root systems may have strong implications for plant fitness and ecosystem functioning (Brunner *et al.*, 2015; Freschet *et al.*, 2021b). In recent decades, large forested regions around the globe have undergone drought- and heatwave-associated decline and mortality (Allen *et al.*, 2010; Hartmann *et al.*, 2018; Hammond *et al.*, 2022). In this regard, in the Mediterranean basin, even tree species as holm oak (*Quercus ilex* L. subsp. *ballota* (Desf.) Samp.) that are well adapted to the Mediterranean conditions have suffered such increased decline (i.e. canopy defoliation; Brasier, 1996; Peñuelas *et al.*, 2001; Carnicer *et al.*, 2011) and mortality since the 1980s. Holm oak decline is characterized by sudden tree death or a gradual loss of foliage that affects the hole crown or just some branches (Camilo-Alves *et al.*, 2013). Furthermore, holm oak decline has been associated with alterations in the physiological (i.e. nonstructural carbohydrates) and structural traits of roots (Villar-Salvador *et al.*, 2004; León *et al.*, 2017). Identifying root functional traits related to tree decline is crucial to define the risk factors of tree mortality and understanding the mechanisms underlying tree decline and death processes (Hartmann *et al.*, 2018).

Warmer and drier conditions are climate change-related factors with potential effects on root functional traits (Brunner *et al.*, 2015). Additionally, the presence of soil-borne pathogens such as *Phytophthora cinammonni* Rands. exacerbates the impact of drought events (Ruiz-Gómez *et al.*, 2019). This pathogen is present worldwide (Scott *et al.*, 2013) and is responsible for fine root rot in holm oak (Corcobado *et al.*, 2013a,b, 2017; Ruíz-Gómez *et al.*, 2015) and thus for diminishing the capacity of the trees to uptake and transport water and essential nutrients to the crown (Jönsson, 2006; Ruiz-Gómez *et al.*, 2019). Once tree physiological damage surpasses a threshold, tree death occurs (Anderegg & Anderegg, 2013). However, before physiological damage is irreversible, trees trigger different strategies, simultaneously (i.e.

anatomical, physiological, chemical, biochemical and molecular), to mitigate such environmental belowground stress. These adjustments occur at the expense of changes in carbon (C) allocation to belowground compartments (i.e. by increasing the root-to-shoot ratio; Brunner & Godbold, 2007; Moser *et al.*, 2015) and by extending the taproots to the deep water level (Barbeta & Peñuelas, 2017), mechanisms that will further affect the morphology and physiology in the fine root system (Zadworny *et al.*, 2021). Such responses occur at the expense of different metabolic substrates such as carbohydrates (Ritchie & Dunlap, 1980; Camisón *et al.*, 2020). Nonetheless, water deprivation may lead to photosynthesis limitation and predispose the tree to car depletion and deficiency (McDowell *et al.*, 2008; Gessler *et al.*, 2018) affecting the availability of carbohydrates and consequently leaf flush (Freschet *et al.*, 2021b) and root growth (Ritchie & Dunlap, 1980; Willaume & Pagès, 2006, 2011), and restricting the use of carbohydrates to respiration and osmoregulation processes (Hartmann *et al.*, 2013). Additionally, the availability of carbohydrates, critical for the development of the root systems, does not depend solely on environmental conditions (i.e. drought) but also on phenological events (i.e. the developmental stage of the tree tissues; leaf flush, flowering or root growth; Willaume & Pagès, 2006; Angay *et al.*, 2014). An alternation between root and shoot development has been observed for different *Quercus* species (Reich *et al.*, 1980; Willaume & Pagès, 2006; Angay *et al.*, 2014), where maximum leaf expansion usually coincides with minimum root growth and vice versa (Reich *et al.*, 1980; Willaume & Pagès, 2006, 2011). In this context, it is essential to better understand the energy costs associated with increased phenotypic plasticity of the tree root system under high-stress conditions and its implications for defoliation.

In this study, we focused on holm oak trees growing in Spanish dehesas. The dehesas are human-shaped savannah-like ecosystems, considered to be among the most threatened ecosystems in Spain (Pulido *et al.*, 2001; Herguido-Sevillano *et al.*, 2017) as a consequence of the interaction between pathogen outbreaks (i.e. *Phytophthora* spp., Brasier, 1996; Solla *et al.*, 2009; Martín-García *et al.*, 2015; Corcobado *et al.*, 2017), climate change-related extreme events (i.e. drought and high temperatures; Allen *et al.*, 2015) and an intensive human management in recent decades due to the abandonment of traditional uses of the dehesa. Specifically, our study focused on investigating the fine root phenotypic plasticity and the potential trade-offs that may occur between the aboveground (i.e. tree defoliation) and belowground (i.e. roots) compartments of holm oaks. The morphology and architecture of roots are determined by genetic factors, soil physicochemical properties (Alameda & Villar, 2012; Giehl & von Wirén, 2014), biotic interactions (Chen *et al.*, 2016), and the availability and distribution patterns of carbohydrates (Ritchie & Dunlap, 1980). The hypotheses of this study are: stress caused by summer drought and *Phytophthora* on the belowground tree compartment leads to potential changes in the resource uptake strategy of fine roots in holm oak trees through alterations in their morphology and architecture; and changes in the resource-uptake capacity of fine roots imply shifts in non-structural carbohydrate resource allocation (i.e. NSC). In other

words, the improvement of soil resource acquisition may be at the expense of maintaining the photosynthetic capacity of the tree and may lead to crown defoliation.

Materials and Methods

Study sites and experimental design

The study was performed in nine dehesas, characterized by a low tree canopy cover (10–25%). These dehesas are situated in south-west Spain (Supporting Information Fig. S1) and were selected based on a previous study (Corcobado, 2013) in which the interaction between drought and *P. cinnamomi* was identified as the main cause of holm oak decline. Further details on the criteria that were used to select the dehesas may be found in Encinas-Valero *et al.* (2022). The selected dehesas are traditionally used for livestock rearing and grazing, the estimated density of cattle being of 0.4 units ha⁻¹ yr⁻¹. The pH of the soil varies from 4 to 7.7. The climate is Mediterranean, being characterized by hot and dry summers and mild winters. Mean monthly temperatures vary from 6.9 ± 0.6°C (January) to 25.0 ± 0.6°C (August), while mean monthly precipitation varies from 29.8 ± 1.2 mm (January) to 10.4 ± 2.1 mm (August) (CRU Ts v.4; Harris *et al.*, 2020; reference period 2019).

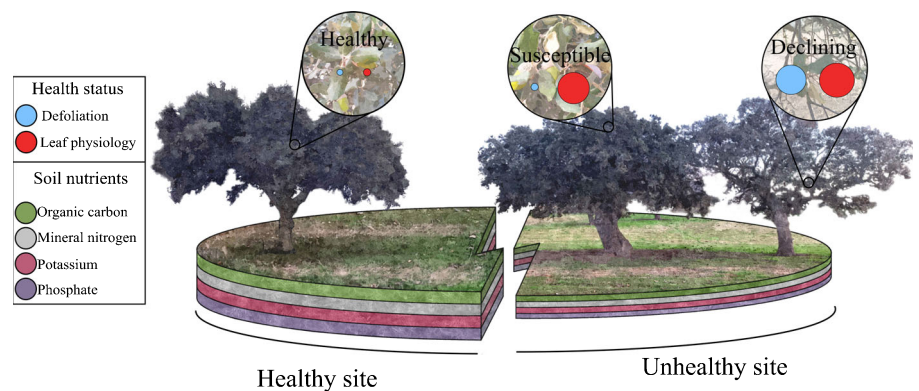
In the nine dehesas, we selected 162 holm oak trees with a mean diameter at breast height of 51.3 ± 1.0 cm and a mean height of 8.4 ± 0.1 m, located in two sampling sites close to each other: a healthy site, where only healthy (i.e. with no apparent crown defoliation) holm oak trees (*n* = 6 per dehesa) were present; and an unhealthy site, where nondefoliated (*n* = 6) and defoliated (*n* = 6) trees were present (Fig. 1). These sampling sites respond to the natural pattern of holm oak decline in dehesas where healthy and unhealthy sites are spatially separated (Brasier, 1992). The a priori visual classification of the health status was later examined by using a three-step protocol. Step 1: crown defoliation of each holm oak was estimated considering the percentage of the total area occupied by the defoliated branches (without leaves) relative to the total crown area of the tree. We used images taken 20 m from the trunks and 1.65 m above the ground that were then analysed using the IMAGEJ software (1.52p; Ferreira & Rasband, 2019; <http://rsbweb.nih.gov/ij/>). Step 2: to further characterize the health status of each holm oak, we

measured Chl_a fluorescence induction, pigments and photoprotective compounds (i.e. chlorophylls, carotenoids and tocopherols, up to now ‘leaf traits’) on fully expanded leaves randomly collected at *c.* 3 m height. The leaf traits used are early stress markers (Esteban *et al.*, 2015; Fenollosa & Munné-Bosch, 2018) that indicate damage at the leaf physiological level and precede the defoliation process. Further details of step 2 may be found in Encinas-Valero *et al.* (2022). Step 3: redundancy analyses (RDA; Fig. S2) using the leaf traits from step 2 were run. Based on RDA of leaf stress markers, we classified the selected holm oak trees into the three health statuses (Fig. 1): healthy, nondefoliated holm oak trees growing in healthy sites and that were characterized by a lower rate of early stress markers in their leaf traits in comparison to the trees from the unhealthy sites (i.e. both nondefoliated and defoliated); susceptible, holm oak trees growing in the unhealthy sites characterized by low defoliation rates (<10% crown defoliation) and a higher rate of early stress markers in comparison to healthy trees; and declining, holm oak trees growing in unhealthy sites characterized by >10% crown defoliation and a higher rate of early stress markers in comparison to healthy trees.

Root and soil sampling

Our target was to collect the shallowest roots of each of the 162 holm oaks. We found a high variability regarding the depth where we could actually collect the roots. This is because the roots of holm oaks in dehesas are found below the roots of the herbaceous compartment, which reach very variable depths (Moreno *et al.*, 2005). We hence defined a sampling protocol that consisted of digging until we were able to collect a representative number of roots sufficient to conduct all our proposed analyses (including nondestructive and destructive analyses, such as NSC). The average sampling depth was 15 cm and generally did not exceed 30 cm depth (most holm oak fine roots, responsible for nutrient uptake, are found in the first 30 cm; Canadell *et al.*, 1992). No significant differences in sample collection depth were found among the health statuses (*P* = 0.7, data not shown). To account for the spatial heterogeneity, the roots were sampled from three random points around the trunks and at a distance of 1 m from them. The three subsamples were then pooled into a single composite sample per each holm oak tree. Soil samples

Fig. 1 Depiction of the health statuses of the holm oak trees and soil nutrient content in each site (i.e. healthy and unhealthy). In detail, the health status is represented by the crown defoliation (blue circle) and the leaf physiology (red circles) (obtained by RDA1, Supporting Information Fig. S2) of the trees. The size of each circle is proportional to the mean crown defoliation and the physiological stress of leaves (group centroid position in RDA1). The soil nutrient content is represented by horizons, in accordance with Table 1, and a thicker soil horizon indicates higher nutrient content.



from the vicinity of the sampled roots were collected following the same protocol. Both roots and soil samples were immediately stored in a portable fridge and maintained at 4°C until they were transported to the laboratory. In the laboratory, soil and root samples were separated into different subsamples to perform different analyses. Soil samples were dried at room temperature (*c.* 20°C), sieved using a 2 mm mesh size and stored in darkness for further analyses. Root samples were gently washed using deionized water to remove the attached residual soil particles and dried, using filter paper. Five to 15 sampled root fragments from each holm oak were then photographed, at a constant distance of 30 cm using a DSLR camera in automatic mode (Eos 1200D; Canon, Amstelveen, the Netherlands), to further characterize their morphology and architecture. Finally, we separated these roots into fine (<2 mm) and coarse (≥ 2 mm), using a digital caliper. Then, we oven-dried all these roots at 60°C for 48 h and subsequently ground them, using a ball mill (MM400; Retsch, Düsseldorf, Germany), until we obtained a fine powder. To avoid rehydration, all ground samples were stored at low humidity conditions (*i.e.* with silica gel in hermetic bags) until further analyses.

Assessment of soil nutrient variables

The soil organic carbon (*i.e.* org. C) content was determined using the dichromate oxidation method described by Walkley & Black (1934) and modified by Yeomans & Bremner (1988). The nitrogen (*i.e.* tot. N) and phosphorus (*i.e.* tot. P) contents were determined based on the Kjeldahl digestion method (Radojevic *et al.*, 1999). Results were expressed as mg of org. C, tot. N or tot. P per 100 mg of soil (%). Ammonium determination was performed based on the modified Berthelot reaction (Krom, 1980; Searle, 1984), while the nitrate and nitrite contents were determined following the cadmium reduction method (Navone, 1964; Walinga *et al.*, 1989). The phosphate soil content was determined following the ammonium-heptamolybdate and potassium antimony oxide tartrate reaction in an acidic medium, using a phosphate solution to form the antimony-phosphomolybdate complex (Boltz & Mellon, 1948), while the potassium soil content was determined at 776 nm by aspirating the sample within a flame (Richards, 1954). Ammonium, nitrate, nitrite, phosphate and potassium results were expressed as $\mu\text{g per g}$ of soil. Finally, the pH of the soil samples was measured through the saturated soil paste method (Kalra, 1995).

Fine root morphological and architectural assessment

All root images were analysed using the image analysis software SMARTROOT (Lobet *et al.*, 2015), a freeware based on IMAGEJ (Ferreira & Rasband, 2019). Specifically, each sampled root fragment was measured using the semiautomatic mode of the SMARTROOT software. The length, surface, volume, diameter and insertion angle of each component of the sampled root fragments were measured. In total, 11 757 root components were measured. These roots were categorized using the following diameter-based classification: fine roots, including roots <0.5 mm in diameter

(class 1), roots 0.5–1 mm in diameter (class 2), roots 1–1.5 mm in diameter (class 3) and roots 1.5–2 mm in diameter (class 4); and coarse roots (≥ 2 mm in diameter). To finally assess the root morphology and architecture of each of the 162 holm oak trees, five parameters were obtained: fine root percentage (FR, %), calculated as the sum of the lengths of the first four classes relative to the sum of the lengths of all the root components (including fine and coarse roots) from the same sample; fine root branching ratio (FRB), calculated as the average of the sum of the ratios between consecutive diameter classes; class 1 : class 2 (*ratio I*) + class 2 : class 3 (*ratio II*) + class 3 : class 4 (*ratio III*) (Chen *et al.*, 2016). This allowed us to estimate the abundance of fine root components relative to thicker fine root components. As our purpose was to obtain a value that summarizes as much as possible the structure of the fine roots, we averaged the three ratios explained above as in Altaf *et al.* (2013). Insertion angle (IA, degrees) was calculated as the mean insertion angle of each of the root components; fine root diameter (FRD, cm) (López *et al.*, 2001) was calculated as the mean diameter of the first four diameter classes; and fine root length (FRL, cm) was quantified as the mean length of the first four diameter classes.

Nonstructural carbohydrate measurements

For all fine (<2 mm) and coarse (≥ 2 mm) sampled roots, nonstructural carbohydrate pools (*i.e.* glucose, fructose, sucrose and starch) were quantified as described in Mariem *et al.* (2020). Briefly, 25 mg of ground root samples was treated with 0.5 ml of 100% ethanol and 0.5 ml of 80% ethanol. These samples were heated in a thermomixer (70°C, 90 min, 1100 rpm) and then centrifuged. The resulting supernatant fractions were used to determine soluble sugars (*i.e.* sucrose, glucose, fructose), using an ion chromatography system (ICS-3000 Dionex; Thermo Scientific, Waltham, MA, USA), after previous sample dilution with water. The starch content was determined in the pellet by adding KOH (0.2 M) and adjusting the pH with acetic acid. The extractions were performed by using a kit that contained amyloglucosidase (R-Biopharm AG, Darmstadt, Germany). The absorbance was measured at 340 nm using a spectrophotometer. The different NSC forms were expressed as mg g^{-1} per dry weight (DW).

Data processing and statistical analyses

To obtain an integrated view of the soil conditions, we performed RDAs using a matrix of data of soil variables including: org. C, tot. N, tot. P, ammonium, nitrate, nitrite, phosphate, potassium and pH (Fig. S3). This matrix was used as the response variable, while the health status of the holm oak (*i.e.* healthy, susceptible and declining) and the 'dehesa' (condition) were used as explanatory variables. For these analyses, we used the 'rda' function from the VEGAN R package (Oksanen *et al.*, 2020).

To define a single variable, we performed principal component analysis (PCA) using all the analysed soil variables logarithmically transformed. For this, we used the 'prcomp' function available in the R base learning functions. Based on the obtained results

(Fig. 2), axis 1 accounted for 48.4% of the variance and was thus used in further analyses as the soil nutrient availability variable.

To test our two hypotheses, we performed two different sets of linear mixed-effects models (LMEs) using the ‘lme’ function available from the NLME R package (Pinheiro *et al.*, 2020): LMEs that included the health status (explanatory variable), and LMEs that included an interaction between a continuous variable and the health status (explanatory variables). The fixed effects of the two sets of LMEs included the response and the explanatory variables, while for the random effect, we used ‘site’ (i.e. healthy and unhealthy) nested within ‘dehesa’ to overcome the experimental design limitation of the two separated sites. To calculate the coefficients of the two sets of LMEs and thus to estimate the effects of each explanatory variable, we ran an ANOVA type III test (available from the CAR R package; Fox & Weisberg, 2019) to deal with the unbalanced design. When significant differences among health statuses of trees were found, we ran a least-square means test based on Tukey HSD, using the EMMEANS R package (Lenth, 2020). All reported LME coefficients were estimated based on the restricted maximum likelihood method (REML). The residuals of the two sets of LMEs were checked for normality using the quantile–quantile plot and the Kolmogorov–Smirnov test. The overall fit of the LMEs was estimated using the pseudo- R^2 (R^2_p ; Nakagawa *et al.*, 2017) whose values represent the coefficient of determination based on the likelihood-ratio test (‘r.squaredLR’ function from the MUMIN R package; Barton, 2020).

For our first hypothesis we used the first set of LMEs to look for differences between the health statuses of trees in soil variables (i.e. org. C, tot. N, tot. P, ammonium, nitrate, nitrite, phosphate, potassium and pH, Table 1) and in the morphology and architecture of roots (i.e. FR, FRB, IA, FRD, FRL). Additionally, a second set of LMEs was used to test for the effects of soil nutrient

availability (i.e. axis 1 of the PCA), health status and their interaction with root morphology and architecture (Table 2; Fig. 3). For each of the morphological and architectural root parameters that responded significantly to the interaction, a phenotypic plasticity index that ranged from zero to one was calculated (Fig. 3). Specifically, we extracted the regression coefficients of the models (Arnold *et al.*, 2019) and used them to predict values at both ends of the soil nutrient availability gradient ($n = 1000$). For that, we considered the confidence intervals calculated by the LME to predict minimum and maximum values. We finally determined this phenotypic plasticity index by calculating the difference between the minimum and maximum values and dividing the obtained result by the maximum value (Valladares *et al.*, 2006). We then performed one-way ANOVAs (i.e. using the ‘t1way’ function from the WRS2 package; Mair & Wilcox, 2018), using the trimmed means, to test for significant differences in terms of phenotypic plasticity index among health statuses. When we found significant differences between health statuses, we performed post-hoc tests using the ‘lincon’ function from the WRS2 package (Mair & Wilcox, 2018). Finally, to represent them graphically, we calculated a mean phenotypic plasticity index for each health status.

For our second hypothesis, a first set of LMEs was used to look for differences in NSC fractions among the health statuses (Fig. 4). Additionally, a second set of LMEs was used to test for the effect of the NSC fractions (i.e. NSC, starch and soluble sugars), health status and their interaction with the parameters of root morphology and architecture (Table S1; Fig. 5). Finally, to evaluate a possible above–belowground trade-off, the tree foliage (the inverse of tree defoliation, see ‘Study sites and experimental design’ in the Materials and Methods section) was divided by FRB, FRD and FRL, separately. We performed LMEs using the

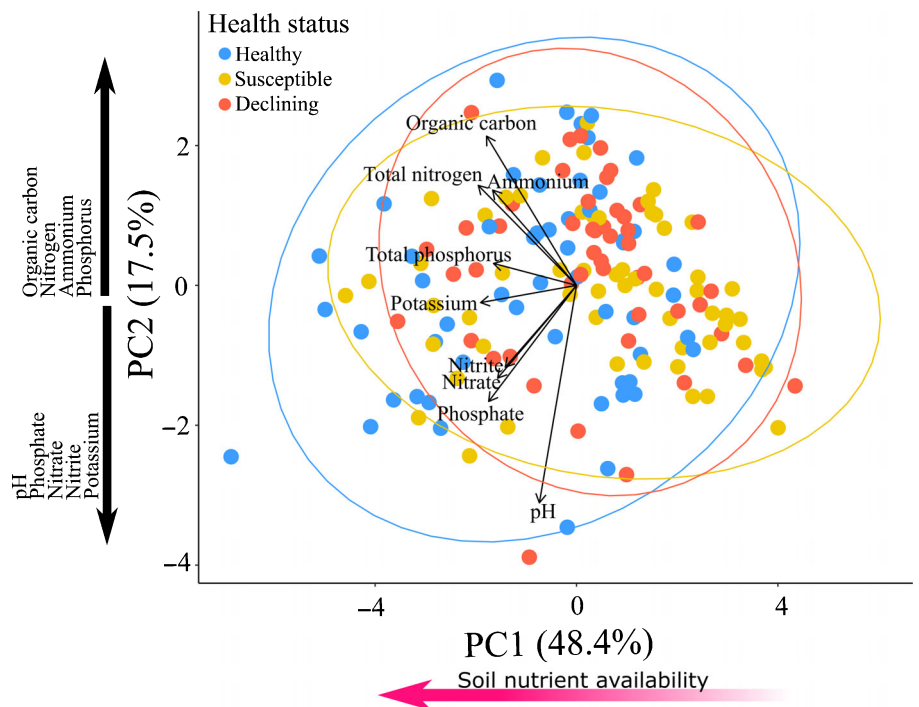


Fig. 2 Results of the principal component analysis (PCAs) run to reduce the number of soil variables and define a single variable (i.e. soil nutrient availability). The soil variables considered were org. C, tot. N, tot. P, ammonium, nitrate, nitrite, phosphate, potassium and pH. Holm oak trees are marked in blue (healthy trees), yellow (susceptible trees) and red (declining trees). Arrows indicate the contribution of the soil variables on each axis.

Table 1 Results of the linear mixed-effects models (LMEs) that tested our first hypothesis: soil pH, nutrients and stoichiometry as a function of the health status (i.e. healthy, susceptible and declining) of holm oak trees.

Variable	Health status			P-value
	Healthy	Susceptible	Declining	
Soil pH	5.56 ± 0.09a	5.53 ± 0.06a	5.49 ± 0.07a	ns
Soil nutrient				
Nitrate ($\mu\text{g g}^{-1}$)	6.11 ± 1.33a	1.81 ± 0.30b	1.62 ± 0.25b	**
Nitrite ($\mu\text{g g}^{-1}$)	0.12 ± 0.04a	0.06 ± 0.01a	0.05 ± 0.01a	ns
Ammonium ($\mu\text{g g}^{-1}$)	3.97 ± 0.81a	2.09 ± 0.20b	2.11 ± 0.23b	**
Phosphate ($\mu\text{g g}^{-1}$)	5.92 ± 1.2a	3.15 ± 0.72b	2.69 ± 0.60b	***
Potassium ($\mu\text{g g}^{-1}$)	84.36 ± 9.31a	57.45 ± 7.65b	52.27 ± 4.38b	***
org. C (%)	2.60 ± 0.16a	2.13 ± 0.16b	2.36 ± 0.16b	*
tot. N (%)	0.16 ± 0.01a	0.13 ± 0.01a	0.14 ± 0.01a	ns
tot. P (%)	0.05 ± 0.004a	0.05 ± 0.007a	0.05 ± 0.005a	ns
Soil stoichiometry				
org. C : tot. N	16.51 ± 0.66a	16.92 ± 0.61a	16.81 ± 0.69a	ns
org. C : tot. P	65.12 ± 5.02a	59.96 ± 3.68a	60.71 ± 4.84a	ns
tot. N : tot. P	3.95 ± 0.22a	3.51 ± 0.19a	3.58 ± 0.22a	ns

Mean ± SE values ($n = 49\text{--}59$) are given for each analysed soil variable. Different letters indicate statistically significant differences (i.e. least-square means based on Tukey HSD tests) between the different health status (healthy, susceptible and declining) of the holm oak trees. Asterisks indicate statistically significant differences: *, $P < 0.05$; **, $P < 0.01$; ***, $P < 0.001$. Bold letters indicates significant differences among the health statuses. Abbreviations for root functional parameters: org. C (%), soil organic carbon; tot. N, total nitrogen; tot. P, total phosphorus. ns, nonsignificant relationships.

Table 2 Effects of soil nutrient availability, health status (healthy, susceptible and declining) and their interaction on the morphology and architecture of the parameters of the holm oak root.

Source of variation	FR (%)			FRB			IA (degrees)			FRD (cm)			FRL (cm)		
	df	χ^2	P-value	df	χ^2	P-value	df	χ^2	P-value	df	χ^2	P-value	df	χ^2	P-value
Intercept	1	248.7	0.000	1	1.991	0.158	1	3316	0.000	1	423.8	0.000	1	153.9	0.000
Soil nutrient availability	1	0.565	0.451	1	3.618	0.057	1	2.002	0.157	1	1.862	0.172	1	1.868	0.171
Health status	2	0.276	0.871	2	1.061	0.588	2	2.548	0.279	2	2.725	0.255	2	2.882	0.236
Soil nutrient availability × Health status	2	0.430	0.806	2	10.27	0.006	2	2.067	0.355	2	9.218	0.009	2	12.41	0.002

Abbreviations for roots functional parameters: FR (%), fine root percentage; FRB, fine root branching; IA (degrees), insertion angle; FRD (cm), fine root diameter; FRL (cm), fine root length. df, degrees of freedom; χ^2 , chi-square statistic. Values in bold indicate significant relationships based on ANOVA type III tests performed along with the linear mixed-effects models (LMEs).

three different foliage : root parameter ratios (response variable) and soil nutrient availability, health status and its interaction (explanatory variables) (Table S2; Fig. 6), and LMEs using the foliage : root parameter ratios (response variable) and health status (explanatory variable) (Fig. 6b,e).

All statistical analyses were performed in R (v.4.0.0; R Core Team, 2020).

Results

Are root parameters affected by soil nutrient availability and the health status of the holm oak trees?

Soil nutrients (i.e. nitrate, ammonium, phosphate, potassium) and organic carbon content were affected by the health status of trees (Table 1). In healthy sites, the soil under healthy trees showed significantly higher values of nitrate ($P < 0.01$),

ammonium ($P < 0.01$), phosphate ($P < 0.001$), potassium ($P < 0.001$) and org. C content ($P < 0.05$) compared to the soil under susceptible and declining trees (Table 1; Fig. 1). The results of this analysis were complemented by those obtained from RDA, which showed a significant effect of the health status of the trees ($R^2 = 0.03$; $P < 0.001$) on the linear combination of the soil variables (i.e. org. C, tot. N, tot. P, nitrite, nitrate, ammonium, potassium, phosphate and pH). The explanatory variables 'dehesa' and 'health status' explained 40% and 4% of the total variation, respectively. On axis 1, nitrate had the highest loading factor (-0.67). On axis 2, nitrate and potassium explained most of the variation; these two variables had the highest (0.11) and the lowest (-0.16) loading factors on this axis, respectively (Fig. S3).

On axis 1 of the PCA, created to integrate soil nutrient availability (i.e. the defined soil nutrient availability variable), tot. N was the variable that had the highest loading factor (-0.39)

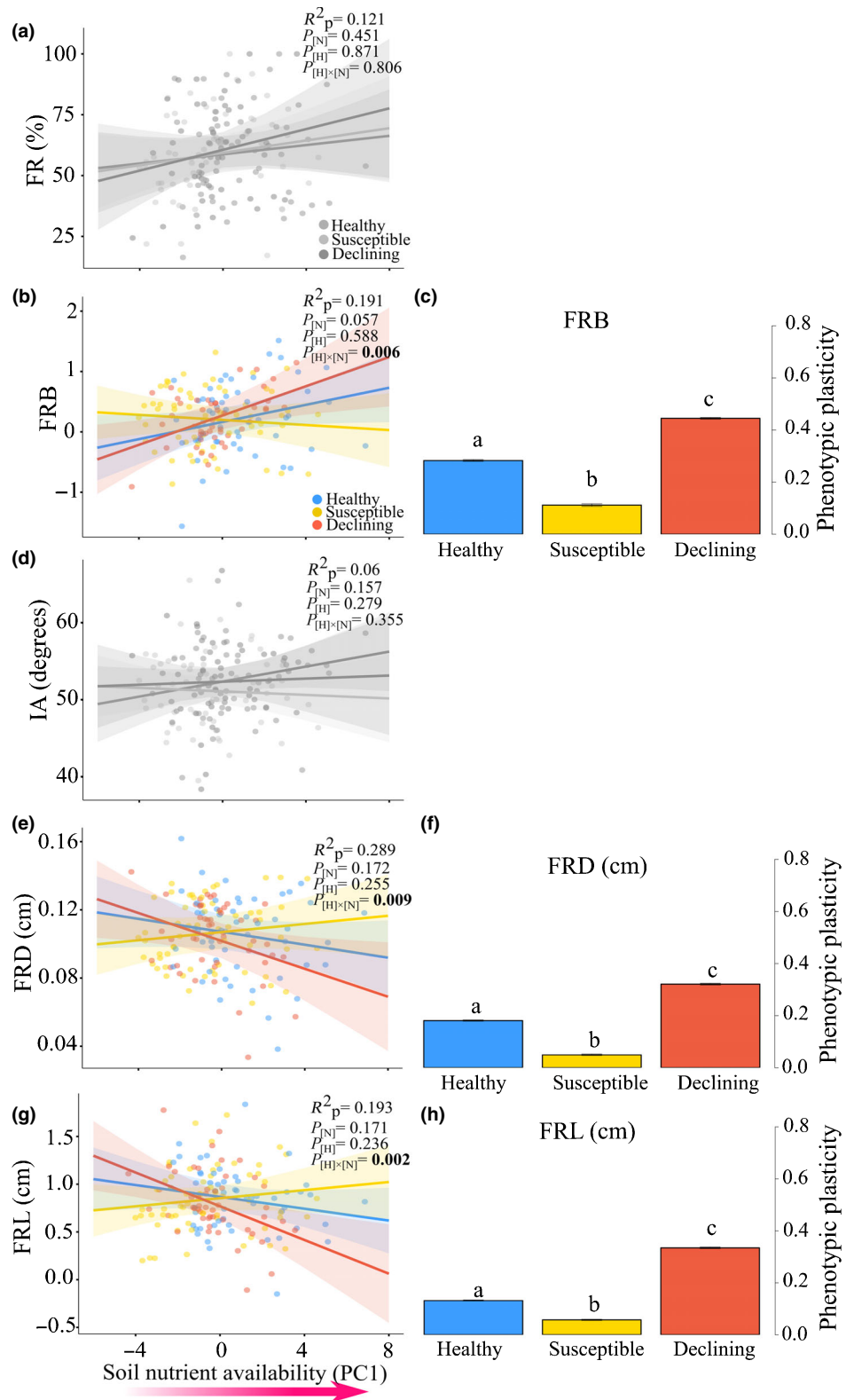


Fig. 3 Results of linear mixed-effects models showing, on the one hand, how the fine root parameters of the holm oak trees respond as a function of soil nutrient availability, health status and their interaction (a, b, d, e, g) and, on the other, how the phenotypic plasticity index varies across health statuses (i.e. when significant effects of the health status are found) (c, f, h). FR (%), fine root percentage; FRB, fine root branching; IA (degrees), insertion angle; FRD (cm), fine root diameter; FRL (cm), fine root length. The soil nutrient availability variable was derived from axis 1 of the PCA (Fig. 2). This component was multiplied by -1 to facilitate comprehension. Solid lines represent the trends of each root parameter along the gradient of soil nutrient availability (i.e. fitted LME values) as a function of health status. The shaded areas represent the 95% confidence intervals. The R_p^2 or fraction of variation explained by the model was calculated according to Nakagawa *et al.* (2017). The phenotypic plasticity, calculated for each health status as described in 'Data processing and statistical analyses' in the Materials and Methods section, is represented by bar plots (mean \pm SE). Different letters indicate significant differences ($P < 0.05$) according to the multiple pairwise comparisons test. Colourless figures (a, d) show nonsignificant LME results.

(Fig. 2). On axis 2, org. C (loading factor = 0.43) and pH (loading factor = -0.63) were the two soil variables that contributed most. Hence, we used this axis to test our first hypothesis (i.e. effects of soil nutrient availability and health status on the root

parameters). The results of the LME that tested our first hypothesis indicated that the interaction between soil nutrient availability and health status affected the morphology and architecture of the fine roots (i.e. FRB, FRD, FRL) of holm oak trees (Table 2;

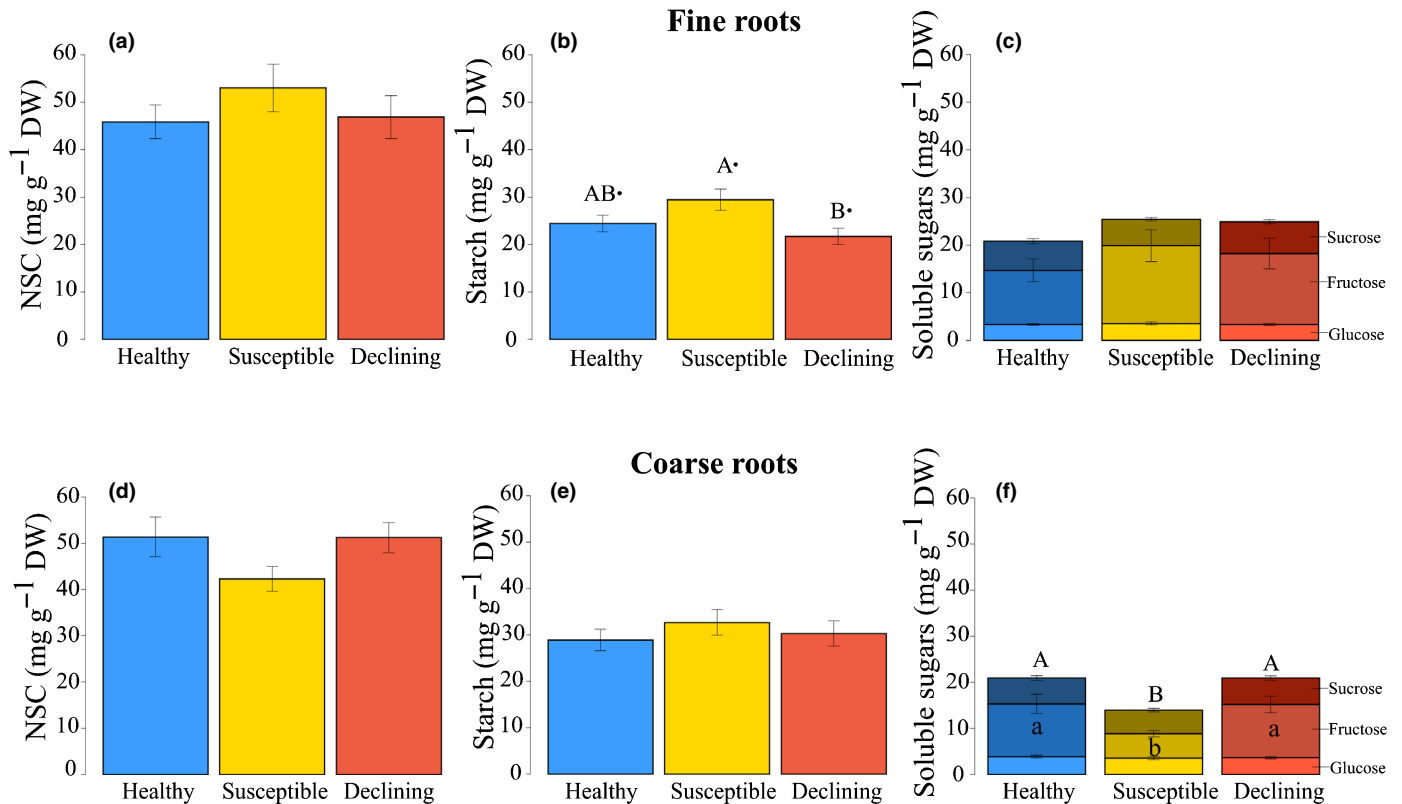


Fig. 4 Total nonstructural carbohydrates (NSC), starch and soluble sugars for fine and coarse roots as a function of health status (healthy, susceptible and declining holm oak trees): that is, total NSC (sum of starch and soluble sugars; a, d), starch (b, e) and soluble sugars (sum of sucrose, fructose and glucose, marked from darker to brighter colours; c, f). Each bar indicates the mean \pm SE of each health status (healthy, $n = 54\text{--}33$; susceptible, $n = 59\text{--}38$; declining $n = 49\text{--}26$). Different uppercase letters indicate statistically significant differences between health statuses of the holm oaks, while different lowercase letters indicate statistically significant differences between the different fractions of the soluble sugars (least-square means based on Tukey HSD tests). Closed points beside the letters indicate marginally significant differences.

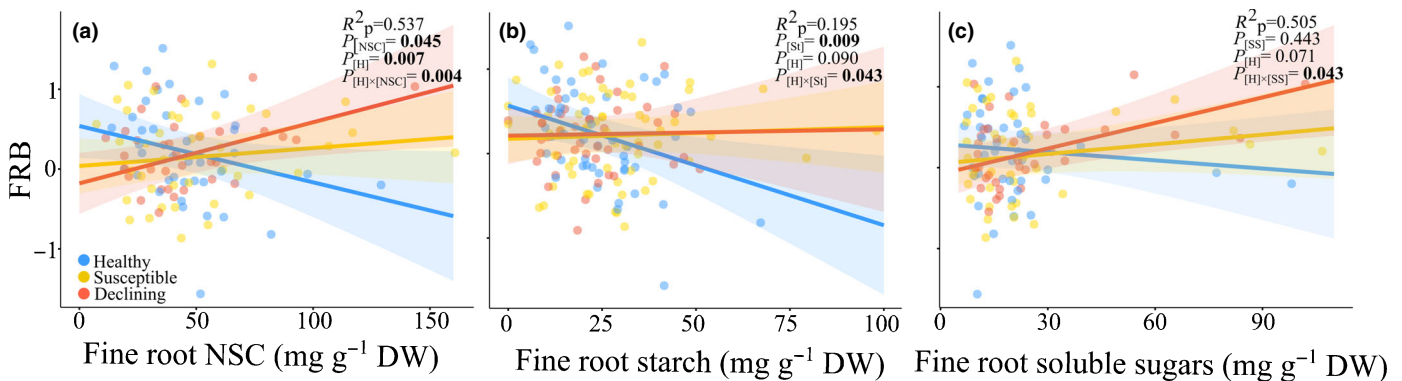
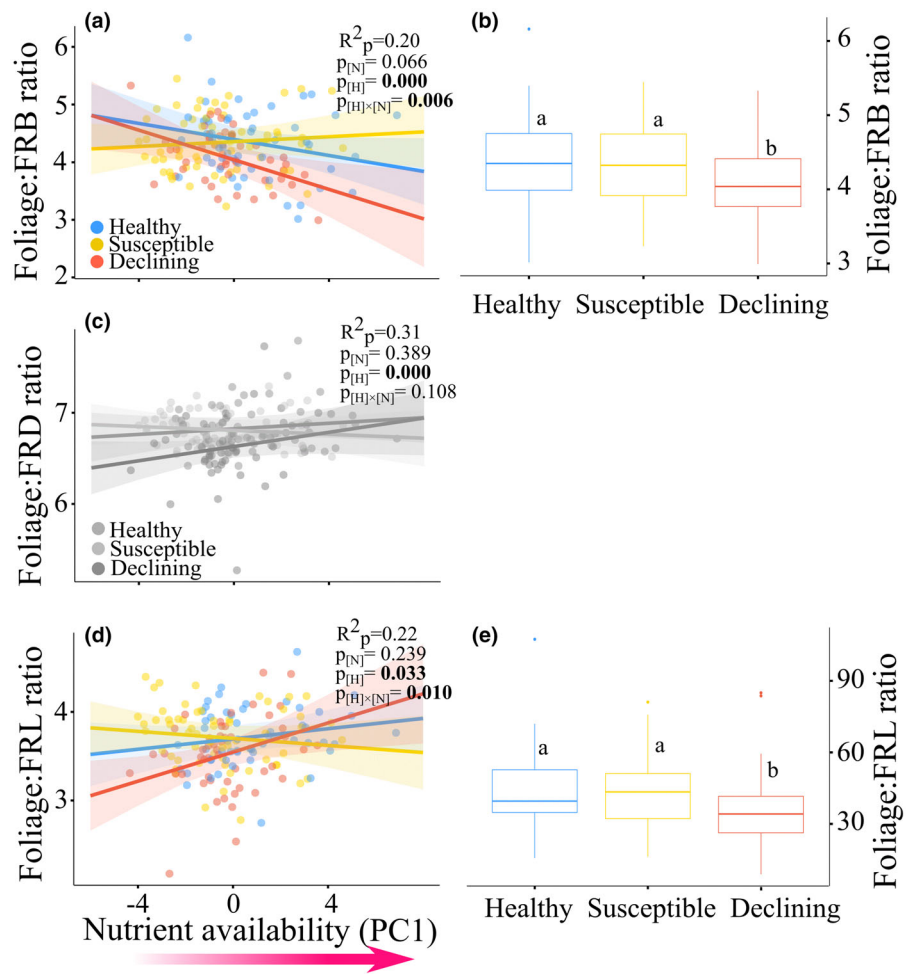


Fig. 5 Linear mixed-effects models of the fine root branching ratio (FRB) as a function of nonstructural carbohydrate fractions, health status and their interaction. FRB was logarithmically transformed to account for normality as a function of NSC (a; $\text{mg g}^{-1} \text{DW}$), starch (b; $\text{mg g}^{-1} \text{DW}$) and soluble sugars (c; $\text{mg g}^{-1} \text{DW}$) of fine roots. Different colours indicate different health statuses of the holm oak trees: that is, blue (healthy trees), yellow (susceptible trees) and red (declining trees). Shaded areas represent the 95% confidence interval. The pseudo- R^2 (R_p^2 ; i.e. the fraction of variation explained by the model) was calculated according to Nakagawa *et al.* (2017).

Fig. 3b,e,g). Specifically, declining trees showed lower FRB values at low soil nutrient availability and higher FRB values at high soil nutrient availability than susceptible and healthy trees (Fig. 3b). Regarding FRD, declining trees showed higher FRD values

under conditions of lower soil nutrient availability and lower FRD values under conditions of higher soil nutrient availability in comparison to susceptible and healthy trees (Fig. 3e). Finally, regarding FRL, declining trees presented longer fine roots under

Fig. 6 Linear mixed-effects models of the foliage : fine root parameter ratio as a function of nutrient availability, health status and its interaction. The fine root parameters represented are fine root branching ratio (FRB, a), fine root diameter (FRD, b) and fine root length (FRL, c). Ratios were logarithmically transformed to fulfil assumptions. Soil nutrient availability is derived from the principal component analysis (PC1; Fig. 2) and multiplied by -1 to facilitate comprehension. The health status of the holm oak trees is marked in blue (healthy), yellow (susceptible) and red (declining) colours. Solid lines represent the trend of each health status along soil nutrient gradient (fitted values). The shaded area represents the 95% confidence interval. R_p^2 (fraction of variation explained by the model) was calculated according to Nakagawa *et al.* (2017). The colourless interaction model represents nonsignificant interactions. Note that the foliage : root parameter ratios are also represented by boxplots (b, e; only for significant interactions). Box represents 50% of the data ($n = 43$ –53 trees per health status) distribution between the first and the third quartile; the central line represents the median; and the upper and lower whiskers cover the 1.5 interquartile range. Different letters indicate significant differences ($P < 0.05$) between the different health statuses on a Tukey multiple pairwise comparisons test.



conditions of low soil nutrient availability and shorter fine roots under conditions of high soil nutrient availability than susceptible and healthy trees (Fig. 3g). Additionally, FRB, FRD and FRL showed a higher phenotypic plasticity in declining than in susceptible and healthy trees (Fig. 3c,f,h).

Does FRB response to tree resource allocation depend on the trees' health status?

NSC fractions did not differ as a function of health status, either for fine or for coarse roots (Fig. 4a,c,d,e) except for fine root starch and coarse root fructose contents (Fig. 4b,f). Specifically, susceptible trees showed marginally higher fine root starch values (28.4 ± 2.2) than declining trees (21.2 ± 1.7) ($P < 0.1$). Coarse roots showed a significantly higher ($P < 0.001$) fructose content in healthy (11.4 ± 2.0) and declining (11.5 ± 1.7) holm oaks than in susceptible ones (5.3 ± 0.6) (Fig. 4f). These differences were also reflected in the total soluble sugar content of the coarse roots, which was significantly higher ($P < 0.001$) in healthy (21.6 ± 2.6) and declining (20.4 ± 2.0) holm oaks than in susceptible ones (13.9 ± 0.9) (Fig. 4f).

The results of the LMEs that tested our second hypothesis showed that FRB responded significantly to the interaction

between NSC, starch or soluble sugars and health status (Fig. 5; Table S1). Specifically, we found that, at higher content of NSC and soluble sugars, FRB in declining trees tended to increase in contrast to healthy trees (Fig. 5a,c). Additionally, at higher content of starch, FRB of trees from the healthy site tended to decrease in contrast to the trees from the unhealthy site (Fig. 5b).

Is there a trade-off in terms of foliage : root ratio considering soil nutrient availability gradient and health status?

The foliage : FRB and foliage : FRL ratios responded significantly to the interaction between health status and soil nutrient availability, while the foliage : FRD ratio showed no response in this regard (Fig. 6; Table S2). Specifically, the foliage : FRB ratio decreased significantly, along the soil nutrient availability gradient, in declining holm oaks compared with healthy ones. Also, susceptible holm oaks exhibited no response at all to the soil nutrient availability gradient (Fig. 6a). In contrast to the foliage : FRB ratio, the foliage : FRL ratio showed lower values at low soil nutrient availability and higher values at high soil nutrient availability in declining trees (Fig. 6d). Finally, regarding the response of the foliage : FRB and foliage : FRL ratios to health

status, we found that declining holm oak trees showed significantly lower values than healthy and susceptible holm oak trees ($P < 0.05$, Fig. 6b,e).

Discussion

Declining holm oak trees showed higher phenotypic plasticity to soil nutrient availability in fine root parameters than susceptible and healthy trees

The results support our first hypothesis that the stress level of the tree (i.e. health status) determined soil resource uptake strategies (Fig. 3) reflected in root morphological and architectural changes. The weak response or absence of response in morphological and architectural fine root parameters of healthy and susceptible holm oak trees along the soil nutrient availability indicated a constant conservative resource uptake strategy. By contrast, when soil nutrient availability was high, declining holm oaks presented more branched fine roots (FRB, Fig. 3b) and consequently a higher number of fine root tips along with thinner (FRD, Fig. 3e) and shorter fine roots (FRL, Fig. 3g) in comparison to healthy and susceptible holm oaks. The responses observed in declining trees may represent an acquisitive strategy (Jia *et al.*, 2013) that would enhance the effective absorbing local root surface and favour soil resource acquisition (Pregitzer, 2008; Beidler *et al.*, 2015; Liese *et al.*, 2017; Yahara *et al.*, 2019; Wambsganss *et al.*, 2021) to counteract the potentially negative effects of drought, defoliation (Gessler *et al.*, 2017) and other indirect factors that reduce soil nutrient uptake, such as the loss of ectomycorrhizal fungi (Corcobado *et al.*, 2015). By contrast, in declining trees under low soil resource availability, few root branches and the presence of thicker and longer fine roots (Fig. 3b,e,g) may favour the exploration of a large volume of soil when resources are limited (Belsky, 1994; Beidler *et al.*, 2015; Eissenstat *et al.*, 2015; Montagnoli *et al.*, 2018). These characteristics are associated with a more conservative resource uptake strategy (Liese *et al.*, 2017; Li *et al.*, 2020).

Overall, three out of the five morphological and architectural fine root parameters analysed here (i.e. FRB, FRD and FRL) were found to be significantly affected by the interaction between soil nutrient availability gradient and the health status of the trees. The large changes in the fine root architecture and morphology in declining trees along the soil nutrient availability revealed a higher fine root phenotypic plasticity in comparison to susceptible and healthy trees (Fig. 3c,f,h). This high phenotypic plasticity suggests that declining holm oaks develop their root systems to cope with the stress to which they are subjected (i.e. drought and root-rot by pathogens such as *Phytophthora*; Corcobado *et al.*, 2013a; Ruiz-Gómez *et al.*, 2019). However, Mediterranean evergreen holm oaks have been reported to exhibit low phenotypic plasticity (Valladares *et al.*, 2000, 2007; Baquedano *et al.*, 2008). Thus, we speculate that the phenotypic plasticity associated with declining trees may not constitute an adaptive advantage (Storz *et al.*, 2021) or an increase in fitness (Bonser, 2021) in the context of the Spanish dehesas. While holm oak trees are well adapted to the harsh environmental conditions where they have evolved

(Moreno & Cubera, 2008; García-Angulo *et al.*, 2020), Spanish dehesas are susceptible when subject to a sequence of different stochastic disturbances, including unusually or extreme long drought, clearing, ploughing, grazing and other anthropic land use-related disturbances that expose holm oak to unpredictable changes in water and nutrient availability (Plieninger, 2006). All these factors may favour lower phenotypic plasticity and thus a conservative resource-use strategy, such as the one we observed in healthy and susceptible holm oak trees (Fig. 3c,f,h), even when the resources are temporarily abundant, to avoid the development of plant structures, too costly to maintain once conditions deteriorate (Baquedano *et al.*, 2008). In addition, conservative root growth in oaks has been reported to be more resilient to pathogen infections and subsequent drought than a more acquisitive and extensive root system (Biocca *et al.*, 1993; Haavik *et al.*, 2015).

Changes in the resource acquisition strategy of the fine roots of declining trees imply a carbon cost

Our results indicated no carbon depletion during the onset of holm oak decline, that is no changes in the overall NSC content as a function of health status (Fig. 4a,d). This implies that carbon availability was not affected by the health status of the holm oak trees and fine roots were not subjected to potential carbon deprivation from photosynthesis limitation (Sanz-Pérez *et al.*, 2009; Zang *et al.*, 2014) and/or from the belowground stressful conditions imposed by root rot pathogens (*P. cinnamomi*) and drought (Corcobado *et al.*, 2013a). Nonetheless, the higher values that we found regarding the fructose content in the coarse roots of the declining trees in comparison to susceptible trees (Fig. 4f) may indicate an osmotic response to enhance water uptake (Dietze *et al.*, 2014; Brunner *et al.*, 2015) or higher respiratory demands (Hartmann & Trumbore, 2016). This is because NSCs are involved in a wide variety of functions such as energy metabolism, growth, osmoregulation, transport, storage, defences and symbiotic interactions (Hartmann & Trumbore, 2016). In addition, the marginally significant decrease of the starch content in the fine roots of the declining holm oak trees in comparison with the fine roots of the susceptible ones (Fig. 4b) may be caused by the decrease of canopy carbon uptake, which in turn may be caused by a decrease in foliage cover and hence in the capacity of the trees to properly photosynthesize (Willaume & Pagès, 2006, 2011; Peguero-Pina *et al.*, 2018).

By analysing the FRB responses to the total NSC, starch and soluble sugar contents (Fig. 5), we found that the total NSC and soluble sugar contents may play an important role in increasing the acquisitive capacity of the fine roots of the declining holm oak trees, which partially confirms our second hypothesis. Specifically, we found a positive relationship between FRB and total NSC and between FRB and the soluble sugar content in declining holm oak trees in contrast to healthy and susceptible trees (Fig. 5a,c). These results highlight the importance of overall NSC and soluble sugars in development of the fine roots under stressful conditions (Ritchie & Dunlap, 1980). This suggests that under scenarios of severe drought stress induced by a pathogen, root branching (FRB) in declining trees may come at the expense

of a high energetic demand (i.e. NSC and soluble sugars) (Ritchie & Dunlap, 1980; Zadworny *et al.*, 2021) to optimize resource acquisition (Dewar *et al.*, 1994; Montagnoli *et al.*, 2018). However, we cannot rule out the possibility that this positive relationship between FRB and overall NSC or soluble sugars may also be explained by the increase in carbon cost associated with the mechanisms of defence against *Phytophthora* (Jönsson, 2006). It has been reported that the severity of *Phytophthora* may increase at high soil nutrient availability (mainly organic matter and nitrate; Broadbent & Baker, 1974; Jönsson, 2006; Corcobado *et al.*, 2013b). Moreover, high values of overall NSC and soluble sugars in secondary fine roots as a result of an acquisitive strategy (declining trees, Fig. 5) have been associated with the success of *Phytophthora* spp. infection in oak roots (Angay *et al.*, 2014).

Trade-offs between foliage maintenance and root exploration strategies as drivers of health status

It has been reported that the maintenance costs of leaves and roots increase under soil stressful conditions (Laureano *et al.*, 2013, 2016). Under these adverse environmental conditions, we observed that declining trees presented a high percentage of crown defoliation (Fig. 1; Encinas-Valero *et al.*, 2022). The observed trade-off between NSC investment in fine root branching associated with defoliation (Fig. 6) further confirms our second hypothesis. Hence, we speculate that in such a demanding environment, where roots are affected by drought and pathogen infection, a shift in holm oak allocation of carbohydrates takes place to maintain a root system architecture and morphology that enhance tree resource acquisition capacity. These changes occur at the expense of maintaining foliage, which results in tree defoliation (Fig. 6a,d). While our results are more qualitative than quantitative (neither fine root nor leaf biomass were measured), they are consistent with previous studies which showed that a greater root investment at the expense of leaf biomass takes place under drought conditions (Dewar *et al.*, 1994; Jacobs *et al.*, 2009; Moser *et al.*, 2015; Ruíz-Gómez *et al.*, 2018), during dry seasons (Montagnoli *et al.*, 2018) and when an infestation of soil-borne pathogens occurs (León *et al.*, 2017; Łakomy *et al.*, 2019; Vivas *et al.*, 2021). Hence, an alternative explanation of phenotypic plasticity could be a potential feedback loop ultimately resulting in tree death that may consist of shifts in the allocation of carbohydrates towards maintaining root functioning at the expense of foliage to cope with stressful conditions (i.e. drought and root rot pathogens). This response is expressed in declining trees, whereas healthy and susceptible trees, not affected by root pathogens (i.e. absent or less virulent), might not suffer enough stress to trigger this root response and negative feedback loop. This would additionally explain why healthy and susceptible trees exhibited low phenotypic plasticity.

Final remarks and conclusions

Our study provides new insights into the mechanisms that underlie decline in holm oak trees growing under conditions of drought and root rot. Our findings suggest that belowground

stress and substantial reduction in the ability of trees to access soil resources determine the architecture and morphology of the root system. To cope with these stressful conditions, a shift in tree NSC allocation is expected to occur to enhance the ability of the radical system to acquire key soil resources at the expense of foliage maintenance, and this ultimately leads to tree death. Hence, climate change, land use, soil resource variability and root rot by pathogens in Spanish dehesas revealed the lack of adaptation of holm oaks in these representative ecosystems of southern Europe. The study further points to the roots as essential elements to define holm oak health, and how roots adapt or not to a changing and harsh environment, and determine holm oak survival in these representative Mediterranean systems. Since dehesas represent a sustainable model of extensive livestock farming, further and urgent research is needed with a focus on how unpredictable environmental conditions can elicit adaptive responses in holm oak roots. A long-term monitoring study that assesses survival rates of trees (i.e. mainly trees with the highest and lowest root phenotypic plasticity) may elucidate whether root responses increase survival chances or lead to tree death. Identification of the resilient phenotypes may lead to the implementation of local breeding programmes with the objective of propagating those individuals capable of coping with the current climatic and biotic environmental challenges faced by dehesa ecosystems. Furthermore, a parallel quantitative assessment of the differences in microbial community structure and functions associated with tree health may help to understand which plant–soil interaction mechanisms are involved in the resistance/vulnerability of holm oak to the environmental stressors under study.










Acknowledgements

We acknowledge the Nutrilab-URJC (Mostoles, Spain) laboratory services for the soil chemical analyses, Dr Iñaki Odriozola for his priceless advice regarding the statistical analyses and the private owners for facilitating access to the sampling dehesas. Thanks to Celia López-Carrasco Fernández and the ‘Consejería de Agricultura, Medioambiente y Desarrollo rural de la Junta de Castilla-la Mancha’ for logistical support. The ‘Tree’ icon by Hey Rabbit Illustrator and ‘Roots’ icon by Guilhem Illustrator, from thenounproject.com were used to design the Graphical abstract. Comments from the anonymous reviewers improved a previous version of the manuscript. This research was mainly funded by the Spanish Government through the IBERYCA project (CGL2017-84723-P), its associated FPI scholarship BES-2014-067971 (ME-V) and SMARTSOIL (PID2020-113244GB-C21). It was further supported by the BC3 María de Maeztu excellence accreditation (MDM-2017-0714; the Spanish Government) and by the BEREC 2018–2021 and the UPV/EHU-GV IT-1018-16 programme (Basque Government). Additionally, this research was further supported through the ‘Juan de la Cierva programme’ (MV; IJCI-2017-34640; the Spanish Government) and one project funded by the Romanian Ministry of Research, Innovation and Digitization through UEFISCDI (A-MH; REASONING, PN-III-P1-1.1-TE-2019-1099).

Author contributions

Research design JCY and RE. Research performance and field sampling ME-V, JCY, RE, A-MH, MV, AS and GM. Analytical measurements ME-V, RE, DF and IA. Data analyses ME-V, JCY and RE. Data interpretation ME-V, JCY and RE; manuscript writing ME-V, JCY and RE; and final writing and revision ME-V, JCY, RE, A-MH, MV, AS, GM and IA.

ORCID

Iker Aranjuelo  <https://orcid.org/0000-0002-8231-5043>
 Jorge Curiel Yuste  <https://orcid.org/0000-0002-3221-6960>
 Manuel Encinas-Valero  <https://orcid.org/0000-0001-9195-283X>
 Raquel Esteban  <https://orcid.org/0000-0003-2560-3310>
 Dorra Fakhet  <https://orcid.org/0000-0003-4344-2645>
 Ana-Maria Hereş  <https://orcid.org/0000-0002-1839-1770>
 Gerardo Moreno  <https://orcid.org/0000-0001-8053-2696>
 Alejandro Solla  <https://orcid.org/0000-0002-2596-1612>
 María Vivas  <https://orcid.org/0000-0003-2712-417X>

Data availability

The data that support the findings of this study are available in the Supporting Information of this article (Dataset S1).

References

- Alameda D, Villar R. 2012. Linking root traits to plant physiology and growth in *Fraxinus angustifolia* Vahl. seedlings under soil compaction conditions. *Environmental and Experimental Botany* 79: 49–57.
- Allen CD, Breshears DD, McDowell NG. 2015. On underestimation of global vulnerability to tree mortality and forest die-off from hotter drought in the Anthropocene. *Ecosphere* 6: 1–55.
- Allen CD, Macalady AK, Chenchouni H, Bachelet D, McDowell N, Venetier M, Kitzberger T, Rigling A, Breshears DD, Hogg EH *et al.* 2010. A global overview of drought and heat-induced tree mortality reveals emerging climate change risks for forests. *Forest Ecology and Management* 259: 660–684.
- Altaf F, Meraj G, Romshoo SA. 2013. Morphometric analysis to infer hydrological behaviour of linder watershed, Western Himalaya, India. *Geography Journal* 2013: 178021.
- Anderegg WRL, Anderegg LDL. 2013. Hydraulic and carbohydrate changes in experimental drought-induced mortality of saplings in two conifer species. *Tree Physiology* 33: 252–260.
- Angay O, Fleischmann F, Recht S, Herrmann S, Matyssek R, Oswald W, Buscot F, Grams T. 2014. Sweets for the foe – effects of nonstructural carbohydrates on the susceptibility of *Quercus robur* against *Phytophthora quercina*. *New Phytologist* 203: 1282–1290.
- Arnold PA, Kruuk LEB, Nicotra AB. 2019. How to analyse plant phenotypic plasticity in response to a changing climate. *New Phytologist* 222: 1235–1241.
- Baquedano FJ, Valladares F, Castillo FJ. 2008. Phenotypic plasticity blurs ecotypic divergence in the response of *Quercus coccifera* and *Pinus halepensis* to water stress. *European Journal of Forest Research* 127: 495–506.
- Barbata A, Peñuelas J. 2017. Increasing carbon discrimination rates and depth of water uptake favor the growth of Mediterranean evergreen trees in the ecotone with temperate deciduous forests. *Global Change Biology* 23: 5054–5068.
- Bardgett RD, Mommer L, De Vries FT. 2014. Going underground: root traits as drivers of ecosystem processes. *Trends in Ecology and Evolution* 29: 692–699.
- Barton K. 2020. Package ‘MUMIN’ title multi-model inference. R package v.1.43.17. [WWW document] URL <https://cran.r-project.org/package=MUMIN> [accessed 1 June 2021].
- Beidler KV, Taylor BN, Strand AE, Cooper ER, Schönholz M, Pritchard SG. 2015. Changes in root architecture under elevated concentrations of CO₂ and nitrogen reflect alternate soil exploration strategies. *New Phytologist* 205: 1153–1163.
- Belsky J. 1994. Influences of trees on savanna productivity: tests of shade, nutrients, and tree-grass competition. *Ecological Society of America* 75: 922–932.
- Berendsen RL, Pieterse CMJ, Bakker PAHM. 2012. The rhizosphere microbiome and plant health. *Trends in Plant Science* 17: 478–486.
- Biocca FH, Tainter DA, Starkey SW, Oak WJG. 1993. The persistence of oak decline in the western north Carolina Nantahala. *Southern Appalachian Botanical Society* 58: 178–184.
- Boltz DF, Mellon MG. 1948. Spectrophotometric determination of phosphorus as molybdiphosphoric acid. *Analytical Chemistry* 20: 749–751.
- Bonsler SP. 2021. Misinterpreting the adaptive value of phenotypic plasticity in studies on plant adaptation to new and variable environments. *Plant Biology* 23: 683–685.
- Brasier CM. 1992. Oak tree mortality in Iberia. *Nature* 360: 539.
- Brasier CM. 1996. *Phytophthora cinnamomi* and oak decline in southern Europe. Environmental constraints including climate change. *Annales des Sciences Forestières* 53: 346–358.
- Broadbent P, Baker KF. 1974. Behaviour of *Phytophthora cinnamomi* in soils suppressive and conducive to root rot. *Australian Journal of Agricultural Research* 25: 121–137.
- Brunner I, Godbold DL. 2007. Tree roots in a changing world. *Journal of Forest Research* 12: 78–82.
- Brunner I, Herzog C, Dawes M, Arend M, Sperisen C. 2015. How tree roots respond to drought. *Frontiers in Plant Science* 6: 1–16.
- Camilo-Alves CS, da Clara M, de Almeida RN. 2013. Decline of Mediterranean oak trees and its association with *Phytophthora cinnamomi*: a review. *European Journal of Forest Research* 132: 411–432.
- Camisón Á, Ángela Martín M, Dorado FJ, Moreno G, Solla A. 2020. Changes in carbohydrates induced by drought and waterlogging in *Castanea sativa*. *Trees* 34: 579–591.
- Canadell J, Djema A, López B, Lloret F, Sabate S, Siscart D, Gracia C. 1992. Structure and dynamics of the root system. In: Roda F, Retana J, Gracia CA, Bellot J, eds. *Ecology of Mediterranean Evergreen Oak Forest*. Berlin & Heidelberg, Germany: Springer-Verlag, 1689–1699.
- Carnicer J, Coll M, Ninyerola M, Pons X, Sánchez G, Peñuelas J. 2011. Widespread crown condition decline, food web disruption, and amplified tree mortality with increased climate change-type drought. *Proceedings of the National Academy of Sciences, USA* 108: 1474–1478.
- Chen W, Koide RT, Adams TS, De Forest JL, Cheng L, Eissenstat DM. 2016. Root morphology and mycorrhizal symbioses together shape nutrient foraging strategies of temperate trees. *Proceedings of the National Academy of Sciences, USA* 113: 8741–8746.
- Corcobado T. 2013. Influencia de *Phytophthora cinnamomi* Rands en el decaimiento de *Quercus ilex* L. y su relación con las propiedades del suelo y las ectomicorrizas. Doctoral dissertation, Universidad de Extremadura, Plasencia, Spain.
- Corcobado T, Cubera E, Moreno G, Solla A. 2013a. *Quercus ilex* forests are influenced by annual variations in water table, soil water deficit and fine root loss caused by *Phytophthora cinnamomi*. *Agricultural and Forest Meteorology* 169: 92–99.
- Corcobado T, Miranda-Torres JJ, Martín-García J, Jung T, Solla A. 2017. Early survival of *Quercus ilex* subspecies from different populations after infections and co-infections by multiple *Phytophthora* species. *Plant Pathology* 66: 792–804.
- Corcobado T, Moreno G, Azul AM, Solla A. 2015. Seasonal variations of ectomycorrhizal communities in declining *Quercus ilex* forests: interactions with topography, tree health status and *Phytophthora cinnamomi* infections. *Forestry* 88: 257–266.
- Corcobado T, Solla A, Madeira MA, Moreno G. 2013b. Combined effects of soil properties and *Phytophthora cinnamomi* infections on *Quercus ilex* decline. *Plant and Soil* 373: 403–413.
- Cubera E, Moreno G, Solla A, Madeira M. 2012. Root system of *Quercus suber* L. seedlings in response to herbaceous competition and different watering and fertilisation regimes. *Agroforestry Systems* 85: 205–214.

- Dewar RC, Ludlow AR, Dougherty PM, Ludlow R, Dewar C, Dougherty PM, Guio S. 1994. Environmental influences on carbon allocation in pines. *Ecological Bulletins* 43: 92–101.
- Dietze MC, Sala A, Carbone MS, Czimczik CI, Mantooth JA, Richardson AD, Vargas R. 2014. Nonstructural carbon in woody plants. *Annual Review of Plant Biology* 65: 667–687.
- Eissenstat DM, Kucharski JM, Zadworny M, Adams TS, Koide RT. 2015. Linking root traits to nutrient foraging in arbuscular mycorrhizal trees in a temperate forest. *New Phytologist* 208: 114–124.
- Encinas-Valero M, Esteban R, Hereş A-M, Becerril JM, García-Plazaola JL, Artexe U, Vivas M, Solla A, Moreno G, Curiel YJ. 2022. Photoprotective compounds as early markers to predict holm oak crown defoliation in declining Mediterranean savannahs. *Tree Physiology* 42: 208–224.
- Esteban R, Barrutia O, Artete U, Fernández-Marín B, Hernández A, García-Plazaola JL. 2015. Internal and external factors affecting photosynthetic pigment composition in plants: a meta-analytical approach. *New Phytologist* 206: 268–280.
- Faucou MP, Houben D, Lambers H. 2017. Plant functional traits: soil and ecosystem services. *Trends in Plant Science* 22: 385–394.
- Fenolosa E, Munné-Bosch S. 2018. Photoprotection and photo-oxidative stress markers as useful tools to unravel plant invasion success. In: Sánchez-Moreiras AM, Reigosa MJ, eds. *Advances in plant ecophysiology techniques*. Cham, Switzerland: Springer International, 153–175.
- Ferreira T, Rasband W. 2019. *IMAGE user guide IJ 1.46r*. [WWW document] URL imagej.nih.gov/ij/docs/guide/ [accessed 10 May 2021].
- Fox J, Weisberg S. 2019. *An R companion to applied regression, 3rd edn*. Thousand Oaks, CA, USA: Sage.
- Freschet GT, Pagès L, Iversen CM, Comas LH, Rewald B, Roumet C, Klimešová J, Zadworny M, Poorter H, Postma JA *et al.* 2021a. A starting guide to root ecology: strengthening ecological concepts and standardising root classification, sampling, processing and trait measurements. *New Phytologist* 232: 973–1122.
- Freschet GT, Roumet C. 2017. Sampling roots to capture plant and soil functions. *Functional Ecology* 31: 1506–1518.
- Freschet GT, Roumet C, Comas LH, Weemstra M, Bengough G, Rewald B, Bardgett RD, De Deyn GB, Johnson D, Klime J *et al.* 2021b. Root traits as drivers of plant and ecosystem functioning: current understanding, pitfalls and future research needs. *New Phytologist* 232: 1123–1158.
- García-Angulo D, Hereş AM, Fernández-López M, Flores O, Sanz MJ, Rey A, Valladares F, Curiel YJ. 2020. Holm oak decline and mortality exacerbates drought effects on soil biogeochemical cycling and soil microbial communities across a climatic gradient. *Soil Biology and Biochemistry* 149: 107921.
- Gazol A, Hereş AM, Curiel YJ. 2021. Land-use practices (coppices and dehesas) and management intensity modulate responses of Holm oak growth to drought. *Agricultural and Forest Meteorology* 297: 108235.
- Gea-Izquierdo G, Montero G, Cañellas I. 2009. Changes in limiting resources determine spatio-temporal variability in tree-grass interactions. *Agroforestry Systems* 76: 375–387.
- Gessler A, Cailleret M, Joseph J, Schönbeck L, Schaub M, Lehmann M, Treydte K, Rigling A, Timofeeva G, Saurer M. 2018. Drought induced tree mortality – a tree-ring isotope based conceptual model to assess mechanisms and predispositions. *New Phytologist* 219: 485–490.
- Gessler A, Schaub M, McDowell NG. 2017. The role of nutrients in drought-induced tree mortality and recovery. *New Phytologist* 214: 513–520.
- Giehl RFH, von Wirén N. 2014. Root nutrient foraging. *Plant Physiology* 166: 509–517.
- Haavik LJ, Billings SA, Guldin JM, Stephen FM. 2015. Emergent insects, pathogens and drought shape changing patterns in oak decline in North America and Europe. *Forest Ecology and Management* 354: 190–205.
- Hammond WM, Williams AP, Abatzoglou JT, Adams HD, Klein T, López R, Sáenz-Romero C, Hartmann H, Breshears DD, Allen CD. 2022. Global field observations of tree die-off reveal hotter-drought fingerprint for Earth's forests. *Nature Communications* 3: 1–11.
- Harris I, Osborn TJ, Jones P, Lister D. 2020. Version 4 of the CRU TS monthly high-resolution gridded multivariate climate dataset. *Scientific Data* 7: 1–18.
- Hartmann H, Moura CF, Anderegg WRL, Ruehr NK, Salmon Y, Allen CD, Arndt SK, Breshears DD, Davi H, Galbraith D *et al.* 2018. Research frontiers for improving our understanding of drought-induced tree and forest mortality. *New Phytologist* 218: 15–28.
- Hartmann H, Trumbore S. 2016. Understanding the roles of nonstructural carbohydrates in forest trees – from what we can measure to what we want to know. *New Phytologist* 211: 386–403.
- Hartmann H, Ziegler W, Trumbore S. 2013. Lethal drought leads to reduction in nonstructural carbohydrates in Norway spruce tree roots but not in the canopy. *Functional Ecology* 27: 413–427.
- Herguido-Sevillano E, Pulido M, Lavado J, Schnabel S. 2017. Spatial patterns of lost and remaining trees in the Iberian wooded rangelands. *Applied Geography* 87: 170–183.
- Jacobs DF, Salifu KF, Davis AS. 2009. Drought susceptibility and recovery of transplanted *Quercus rubra* seedlings in relation to root system morphology. *Annals of Forest Science* 66: 1–12.
- Jia S, McLaughlin NB, Gu J, Li X, Wang Z. 2013. Relationships between root respiration rate and root morphology, chemistry and anatomy in *Larix gmelinii* and *Fraxinus mandshurica*. *Tree Physiology* 33: 579–589.
- Jönsson U. 2006. A conceptual model for the development of *Phytophthora* disease in *Quercus robur*. *New Phytologist* 171: 55–68.
- Kalra YP. 1995. Determination of pH of soils by different methods: collaborative study. *Journal of AOAC International* 78: 310–324.
- Krom MD. 1980. Spectrophotometric determination of ammonia: a study of a modified Berthelot reaction using salicylate and dichloroisocyanurate. *The Analyst* 105: 305–316.
- Kumordzi BB, Aubin I, Cardou F, Shipley B, Violle C, Johnstone J, Anand M, Arsenault A, Bell FW, Bergeron Y *et al.* 2019. Geographic scale and disturbance influence intraspecific trait variability in leaves and roots of North American understory plants. *Functional Ecology* 33: 1771–1784.
- Łakomy P, Kuźmiński R, Mucha J, Zadworny M. 2019. Effects of oak root pruning in forest nurseries on potential pathogen infections. *Forest Pathology* 49: 1–11.
- Langley A, Chapman SK, Hungate BA. 2006. Ectomycorrhizal colonization slows root decomposition: the post-mortem fungal legacy. *Ecology Letters* 9: 955–959.
- Laureano RG, García-Nogales A, Seco JI, Rodríguez JGP, Linares JC, Martínez F, Merino J. 2013. Growth and maintenance costs of leaves and roots in two populations of *Quercus ilex* native to distinct substrates. *Plant and Soil* 363: 87–99.
- Laureano RG, García-Nogales A, Seco JI, Linares JC, Martínez F, Merino J. 2016. Plant maintenance and environmental stress. Summarising the effects of contrasting elevation, soil, and latitude on *Quercus ilex* respiration rates. *Plant and Soil* 409: 389–403.
- Lenth R. 2020. *EMMEANS: estimated marginal means, aka least-squares means*. R package v.1.4.6, R 695 package v.1.4.6. [WWW document] URL <https://cran.r-project.org/package=emmeans> [accessed 13 January 2022].
- León I, García JJ, Fernández M, Vázquez-Piqué J, Tapias R. 2017. Differences in root growth of *Quercus ilex* and *Quercus suber* seedlings infected with *Phytophthora cinnamomi*. *Silva Fennica* 51: 1–12.
- Li J, Attallah K, Wang J, Yu D, Yang Y, Yang L, Lu Z. 2020. Root traits determine variation in nonstructural carbohydrates (NSCs) under different drought intensities and soil substrates in three temperate tree species. *Forests* 11: 415.
- Liese R, Alings K, Meier IC. 2017. Root branching is a leading root trait of the plant economics spectrum in temperate trees. *Frontiers in Plant Science* 8: 315.
- Lobet G, Pound MP, Diener J, Pradal C, Draye X, Godin C, Javaux M, Leitner D, Meunier F, Nacry P *et al.* 2015. Root system markup language: toward a unified root Architecture description language. *Plant Physiology* 167: 617–627.
- López B, Sabaté S, Gracia CA. 2001. Vertical distribution of fine root density, length density, area index and mean diameter in a *Quercus ilex* forest. *Tree Physiology* 21: 555–560.
- Mair P, Wilcox R. 2018. Robust statistical methods using *wrs2*. *Journal of Statistical Software* 52: 464–488.
- Makita N, Hirano Y, Mizoguchi T, Kominami Y, Dannoura M, Ishii H, Finér L, Kanazawa Y. 2011. Very fine roots respond to soil depth: biomass allocation, morphology, and physiology in a broad-leaved temperate forest. *Ecological Research* 26: 95–104.
- Marañón T, Navarro-Fernández CM, Gil-Martínez M, Domínguez MT, Madejón P, Villar R. 2020. Variation in morphological and chemical traits of

- Mediterranean tree roots: linkage with leaf traits and soil conditions. *Plant and Soil* 449: 389–403.
- Mariem SB, Gámez AL, Larraya L, Fuertes-Mendizabal T, Cañameras N, Arous JL, McGrath SP, Hawkesford MJ, Murua CG, Gaudeul M *et al.* 2020. Assessing the evolution of wheat grain traits during the last 166 years using archived samples. *Scientific Reports* 10: 1–13.
- Martín-García J, Solla A, Corcobado T, Siasou E, Woodward S. 2015. Influence of temperature on germination of *Quercus ilex* in *Phytophthora cinnamomi*, *P. gonapodyides*, *P. quercina* and *P. psychrophila* infested soils. *Forest Pathology* 45: 215–223.
- McCormack LM, Adams TS, Smithwick EAH, Eissenstat DM. 2012. Predicting fine root lifespan from plant functional traits in temperate trees. *New Phytologist* 195: 823–831.
- McDowell N, Pockman WT, Allen CD, Breshears DD, Cobb N, Kolb T, Plaut J, Sperry J, West A, Williams DG *et al.* 2008. Mechanisms of plant survival and mortality during drought: why do some plants survive while others succumb to drought? *New Phytologist* 178: 719–739.
- Montagnoli A, Kasten Dumroese R, Terzaghi M, Onelli E, Scipia GS, Chiatante D. 2018. Seasonality of fine root dynamics and activity of root and shoot vascular cambium in a *Quercus ilex* L. forest (Italy). *Forest Ecology and Management* 431: 26–34.
- Moreno G, Cubera E. 2008. Impact of stand density on water status and leaf gas exchange in *Quercus ilex*. *Forest Ecology and Management* 254: 74–84.
- Moreno G, Obrador JJ, Cubera E, Dupraz C. 2005. Fine root distribution in dehesas of Central-Western Spain. *Plant and Soil* 277: 153–162.
- Moser B, Kipfer T, Richter S, Egli S, Wohlgenuth T. 2015. Drought resistance of *Pinus sylvestris* seedlings conferred by plastic root architecture rather than ectomycorrhizal colonisation. *Annals of Forest Science* 72: 303–309.
- Mou P, Jones RH, Tan Z, Bao Z, Chen H. 2013. Morphological and physiological plasticity of plant roots when nutrients are both spatially and temporally heterogeneous. *Plant and Soil* 364: 373–384.
- Nakagawa S, Johnson PCD, Schielzeth H. 2017. The coefficient of determination R² and intra-class correlation coefficient from generalized linear mixed-effects models revisited and expanded. *Journal of the Royal Society Interface* 14: 20170213.
- Navone R. 1964. Proposed method for nitrate in potable waters. *Journal – American Water Works Association* 56: 781–783.
- Oksanen J, Blanchet FG, Friendly M, Kindt R, Legendre P, Mcglinn D, Minchin PR, O'hara RB, Simpson GL, Solymos P *et al.* 2020. *VEGAN: Community ecology package*. R package v.2.5-7. [WWW document] URL <https://cran.r-project.org/package=vegan> [accessed 17 January 2022].
- Peguero-Pina JJ, Mendoza-Herrer Ó, Gil-Pelegrín E, Sancho-Knapik D. 2018. Cavity limits the recovery of gas exchange after severe drought stress in Holm Oak (*Quercus ilex* L.). *Forests* 9: 443.
- Peñuelas J, Lloret F, Montoya R. 2001. Severe drought effects on Mediterranean woody flora in Spain. *Forest Science* 47: 2001.
- Pinheiro J, Bates D, DebRoy S, Sarkar D, Team RC. 2020. *NLME: Linear and nonlinear mixed effects models*. R package v.3.1-148. [WWW document] URL <https://cran.r-project.org/package=nlme> [accessed 17 January 2022].
- Plieninger T. 2006. Habitat loss, fragmentation, and alteration. Quantifying the impact of land-use changes on a Spanish dehesa landscape by use of aerial photography and GIS. *Landscape Ecology* 21: 91–105.
- Poorter H, Ryser P. 2015. The limits to leaf and root plasticity: what is so special about specific root length? *New Phytologist* 206: 1188–1190.
- Pregitzer KS. 2008. Tree root architecture – form and function. *New Phytologist* 180: 552–564.
- Pulido F, Díaz M, Sebastian J. 2001. Size structure and regeneration of Spanish holm oak *Quercus ilex* forests and dehesas: effects of agroforestry use on their long-term sustainability. *Forest Ecology and Management* 146: 1–13.
- R Core Team. 2020. *A language and environment for statistical computing*. Vienna, Austria: R Foundation for Statistical Computing. [WWW document] URL <http://www.r-project.org/> [accessed 9 May 2022].
- Radojevic M, Bashkin V, Bashkin V. 1999. *Practical environmental analysis*. Cambridge, UK: Royal Society of Chemistry.
- Reich PB, Teskey R, Johnson PS, Hinckley TM. 1980. Periodic root and shoot growth in oak. *Forest Science* 26: 590–598.
- Richards LA. 1954. Diagnosis and improvement of saline and alkali soils. *Soil Science* 78: 154.
- Ritchie G, Dunlap J. 1980. Root growth potential: its development and expression in forest tree seedlings. *New Zealand Journal of Forestry Science* 10: 218–248.
- Ruess RW, Hendrick RL, Burton AJ, Pregitzer KS, Sveinbjornsson B, Allen MF, Maurer GE. 2003. Coupling fine root dynamics with ecosystem carbon cycling in black spruce forests of interior Alaska. *Ecological Monographs* 73: 643–662.
- Ruiz-Gómez F, Navarro-Cerrillo RM, Sánchez-Cuesta R, Pérez-de-Luque A. 2015. Histopathology of infection and colonization of *Quercus ilex* fine roots by *Phytophthora cinnamomi*. *Plant Pathology* 64: 605–616.
- Ruiz-Gómez F, Pérez-de-Luque A, Sánchez-Cuesta R, Quero JL, Cerrillo RMN. 2018. Differences in the response to acute drought and *Phytophthora cinnamomi* infection in *Quercus ilex* L. seedlings. *Forests* 9: 1–16.
- Ruiz-Gómez FJ, Pérez-de-Luque A, Navarro-Cerrillo RM. 2019. The involvement of *Phytophthora* root rot and drought stress in Holm Oak decline: from ecophysiology to microbiome influence. *Current Forestry Reports* 5: 251–266.
- Sanz-Pérez V, Castro-Díez P, Joffre R. 2009. Seasonal carbon storage and growth in Mediterranean tree seedlings under different water conditions. *Tree Physiology* 29: 1105–1116.
- Scott P, Burgess T, Hardy GES. 2013. Globalization and Phytophthora. In: Lamour K, ed. *Phytophthora: a global perspective, vol. 2*. Croydon, UK: CPI Group (UK), 226–232.
- Searle PL. 1984. The Berthelot or Indophenol reaction and its use in the analytical chemistry of nitrogen. A review. *Analyst* 109: 549–568.
- Solla A, García L, Pérez A, Cordero A, Cubera E, Moreno G. 2009. Evaluating potassium phosphonate injections for the control of *Quercus ilex* decline in SW Spain: implications of low soil contamination by *Phytophthora cinnamomi* and low soil water content on the effectiveness of treatments. *Phytoparasitica* 37: 303–316.
- Stotz GC, Salgado-Luarte C, Escobedo VM, Valladares F, Gianoli E. 2021. Global trends in phenotypic plasticity of plants. *Ecology Letters* 24: 2267–2281.
- Suseela V, Tharayil N, Orr G, Hu D. 2020. Chemical plasticity in the fine root construct of *Quercus* spp. varies with root order and drought. *New Phytologist* 228: 1835–1851.
- Trubat R, Cortina J, Vilagrosa A. 2012. Root architecture and hydraulic conductance in nutrient deprived *Pistacia lentiscus* L. seedlings. *Oecologia* 170: 899–908.
- Valladares F, Gianoli E, Gómez JM. 2007. Ecological limits to plant phenotypic plasticity. *New Phytologist* 176: 749–763.
- Valladares F, Martínez-Ferri E, Balaguer L, Pérez-Corona E, Manrique E. 2000. Low leaf-level response to light and nutrients in Mediterranean evergreen oaks: a conservative resource-use strategy? *New Phytologist* 148: 79–91.
- Valladares F, Sanchez-Gomez D, Zavala MA. 2006. Quantitative estimation of phenotypic plasticity: bridging the gap between the evolutionary concept and its ecological applications. *Journal of Ecology* 94: 1103–1116.
- Villar-Salvador P, Planelles R, Oliet J, Penuelas-Rubira JL, Jacobs DF, Gonzalez M. 2004. Drought tolerance and transplanting performance of holm oak (*Quercus ilex*) seedlings after drought hardening in the nursery. *Tree Physiology* 24: 1147–1155.
- Vivas M, Hernández J, Corcobado T, Cubera E, Solla A. 2021. Transgenerational induction of resistance to *Phytophthora cinnamomi* in holm oak. *Forests* 12: 100.
- Walinga I, Van Der Lee JJ, Houba VJG, Van Vark W, Van Der Lee JJ. 1989. Part 7. In: *Plant analysis procedure*. Wageningen Agricultural University, Syllabus, 197–200.
- Walkley A, Black IA. 1934. An examination of the Degtjareff method for determining soil organic matter, and a proposed modification of the chromic acid titration method. *Soil Science* 37: 29–38.
- Wambansang J, Freschet GT, Beyer F, Goldmann K, Prada-Salcedo LD, Scherer-Lorenzen M, Bauhus J. 2021. Tree species mixing causes a shift in fine-root soil exploitation strategies across European forests. *Functional Ecology* 35: 1886–1902.
- Willaume M, Pagès L. 2006. How periodic growth pattern and source/sink relations affect root growth in oak tree seedlings. *Journal of Experimental Botany* 57: 815–826.

- Willlaume M, Pagès L. 2011. Correlated responses of root growth and sugar concentrations to various defoliation treatments and rhythmic shoot growth in oak tree seedlings (*Quercus pubescens*). *Annals of Botany* 107: 653–662.
- Yahara H, Tanikawa N, Okamoto M, Makita N. 2019. Characterizing fine-root traits by species phylogeny and microbial symbiosis in 11 co-existing woody species. *Oecologia* 191: 983–993.
- Yeomans JC, Bremner JM. 1988. A rapid and precise method for routine determination of organic carbon in soil. *Communications in Soil Science and Plant Analysis* 19: 1467–1476.
- Zadworny M, Mucha J, Jagodziński AM, Kościelniak P, Łakomy P, Modrzejewski M, Ufnalski K, Żytkowiak R, Comas LH, Rodríguez-Calcerrada J. 2021. Seedling regeneration techniques affect root systems and the response of *Quercus robur* seedlings to water shortages. *Forest Ecology and Management* 479: 118552.
- Zang U, Goisser M, Häberle K-H, Matussek R, Matzner E, Borken W. 2014. Effects of drought stress on photosynthesis, rhizosphere respiration, and fine-root characteristics of beech saplings: a rhizotron field study. *Journal of Plant Nutrition and Soil Science* 177: 168–177.

Supporting Information

Additional Supporting Information may be found online in the Supporting Information section at the end of the article.

Dataset S1 Details of the experimental design, root parameters and soil variables used in this study.

Fig. S1 Location of the nine studied dehesas within the central–western part of the Iberian Peninsula.

Fig. S2 Redundancy analysis (RDA) plot conducted with leaf traits. Boxplot of defoliation of the different health statuses.

Fig. S3 Redundancy analysis (RDA) plot conducted with soil variables.

Table S1 Linear mixed-effects models (LMEs) in which fine root branching ratio (FRB) varied as a function of the different carbohydrate fractions, health status and the interaction between carbohydrate fractions \times health status.

Table S2 Linear mixed-effects models (LMEs) in which foliage : root parameter ratios varied as a function of soil nutrient availability, health status and the interaction between soil nutrient availability \times health status.

Please note: Wiley Blackwell are not responsible for the content or functionality of any Supporting Information supplied by the authors. Any queries (other than missing material) should be directed to the *New Phytologist* Central Office.



About New Phytologist

- *New Phytologist* is an electronic (online-only) journal owned by the New Phytologist Foundation, a **not-for-profit organization** dedicated to the promotion of plant science, facilitating projects from symposia to free access for our Tansley reviews and Tansley insights.
- Regular papers, Letters, Viewpoints, Research reviews, Rapid reports and both Modelling/Theory and Methods papers are encouraged. We are committed to rapid processing, from online submission through to publication 'as ready' via *Early View* – our average time to decision is <23 days. There are **no page or colour charges** and a PDF version will be provided for each article.
- The journal is available online at Wiley Online Library. Visit www.newphytologist.com to search the articles and register for table of contents email alerts.
- If you have any questions, do get in touch with Central Office (np-centraloffice@lancaster.ac.uk) or, if it is more convenient, our USA Office (np-usaoffice@lancaster.ac.uk)
- For submission instructions, subscription and all the latest information visit www.newphytologist.com